

Simultaneous effect of fluorine impregnation on highly mesoporous activated carbon used in high-performance electrical double layer capacitors



Kue-Ho Kim, Jung Soo Lee, Hyo-Jin Ahn*

Department of Materials Science and Engineering, Seoul National University of Science and Technology, Seoul 01811, Republic of Korea

ARTICLE INFO

Keywords:
Electrical double-layer capacitors
Rate-performance
Activated carbon
Mesoporous structure
Fluorine-doped carbon

ABSTRACT

Owing to the increase in need for high-performance energy storage devices, activated carbon has attracted considerable attention as an electrode material for electrical double-layer capacitors (EDLCs). However, the conventional manufacturing process of activated carbon is seriously limited by the depletion of raw material sources. Biomass-based activated carbon, which is currently considered as a breakthrough, exhibits performance limitations such as low specific capacitance and poor high-rate performance. In this study, we propose the use of fluorine-doped mesoporous carbon (F-MAC), which is derived from Ecklonia cava using fluorine impregnation and KOH activation, to address the above challenges. F-MAC exhibits high specific capacitance (184 F/g), excellent high-rate performance (155 F/g at a current density of 20 A/g), and superior cycle stability (82.8% capacitance retention after 2,000 cycles). These performance improvements are attributed to the increased surface area, high mesopore volume fraction, fluorine-doping effect, and high concentration of oxygen functional groups.

1. Introduction

The emergence of global energy issues has necessitated the development of high-performance energy storage devices based on electrochemical reactions, which have advantages such as high energy efficiency and low environmental pollution. In particular, electrochemical capacitors (ECs) have attracted considerable attention due to their excellent cycling stability, fast charge/discharge rate, high power density, and low maintenance cost [1–3]. Electrical double-layer capacitor (EDLC), which is a type of ECs, uses a non-faradaic charge adsorption/desorption process at the interface of the electrolyte and electrode material. EDLCs generally use activated carbon as the electrode material because of their large specific surface area. Activated carbon is generally obtained from depletable sources such as coals, cokes, and pitches [4,5]. Therefore, to prevent the depletion of these source materials, biomass-based activated carbon is currently being considered as a substitute. Activated carbon derived from biomass has distinctive merits such as abundance of raw material, low cost, eco-friendliness, and a simple manufacturing process [6,7]. Owing to these advantages, various raw materials such as corn grain, coconut, jujube, and garlic skin are being used to develop the electrode of high-

performance EDLCs [8–11]. Recently, raw materials extracted from submarine plants such as seaweed, Undaria pinnatifida, and Ecklonia cava (EC) have attracted considerable attention due to their abundance and inherent rich oxygen content [12]. Despite these advantages, biomass-based activated carbon has inferior high-rate performance. This is due to the limitations of the long ionic diffusion pathway, which result in a low mesopore volume fraction.

To overcome this critical drawback, we propose the use of fluorine-doped mesoporous activated carbon (F-MAC) with a high mesopore volume fraction, derived from EC. This mesoporous carbon structure is developed by simultaneous fluorine impregnation with the potassium hydroxide (KOH) activation process. Fluorine impregnation of stabilized EC not only accelerates KOH activation with carbon fluoride generation/decomposition, but also develops a fluorine-doped carbon structure.

2. Experimental details

F-MAC was successfully derived from EC by consecutively performing impregnation and activation. The EC, which was purchased from Jungbu Co. (Korea), was stabilized at 400 °C for 3 h after cleaning with nitric acid (HNO_3 , JUNSEI) to remove the impurities. The stabilized EC

* Corresponding author.

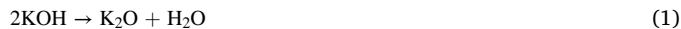
E-mail address: hjahn@seoultech.ac.kr (H.-J. Ahn).

was impregnated with 5 M ammonium fluoride (NH_4F , Aldrich) solution for 12 h and dried in an oven at 80 °C. Subsequently, the dried sample was mixed with KOH (SAMCHUN) at a 1:4 ($W_{\text{sample}}/W_{\text{KOH}}$) weight ratio and carbonized at 800 °C for KOH activation. The resultant samples were washed with hydrochloric acid (HCl, SAMCHUN) and deionized water to remove the activation reaction residue. For comparison, we also prepared carbon derived from EC without KOH activation and fluorine impregnation, with only KOH activation, and with only fluorine impregnation (hereinafter referred to as pristine carbon (PC), activated carbon (AC), and fluorine-doped pristine carbon (F-PC), respectively).

The surface morphology of the sample was observed using field-emission scanning electron microscopy (FESEM, Hitachi S-4800), and the chemical bonding states were investigated through X-ray photoelectron spectroscopy (XPS, ESCALAB 250). To study the porous structure, Brunauer, Emmett, and Teller (BET) and Barrett, Joyner, and Halenda (BJH) analyses were conducted with N_2 adsorption. The Electrochemical performances were evaluated by a two-electrode symmetric system with 6 M KOH electrolyte and nickel foam using a potentiostat/galvanostat (Ecochemie Autolab, PGST302N).

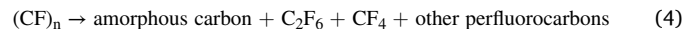
3. Results and discussion

Fig. 1a,b show the image of dried EC and successfully carbonized F-MAC. **Fig. 1c-f** show the FESEM images of PC, AC, F-PC, and F-MAC, respectively. In the case of PC, a relatively smooth surface without any pores can be observed (see **Fig. 1c**). In contrast, the other samples (**Fig. 1d-f**) exhibited porous structures having different pore sizes and pore distributions. It is well known that the pore structure of AC results from the KOH activation process carbonization (see Eqs. (1)-(3)) [13,14]:



The porous structure of the AC obtained from KOH activation is shown in **Fig. 1d**. This method is currently used for the fabrication of

carbon electrodes in EDLCs. In addition, we performed the fluorine impregnation process with stabilized EC as a different approach to create the mesopore structure of carbon. This process is based on the following equation, which causes the generation and decomposition of carbon fluoride during carbonization (see Eq. (4)) [15,16]:



F-PC exhibited a mesoporous structure of carbon with F-doping, as shown in **Fig. 1e**. Interestingly, F-MAC (**Fig. 1f**) exhibited an optimized mesoporous structure, which implies that the introduction of fluorine impregnation and KOH activation had a synergistic effect, resulting in the development of the improved mesoporous structure. This result indicates that the generation and decomposition of carbon fluoride effectively boosted the KOH activation process thereby securing a reaction site on the carbon surface.

Fig. 2 presents the XPS data of all the samples that were used to investigate the chemical binding states. All the binding energy levels were arranged using the binding energy of C 1 s (284.5 eV) as a reference. **Fig. 2a** illustrates the C 1 s XPS core-level spectra, which shows that all the samples possessed the binding energies of C-C groups (at 284.5 eV), C-O groups (at 286.1 eV), C=O groups (at 287.1 eV), and O—C=O groups (at 288.6 eV). Furthermore, the C-O and C=O groups corresponded to the hydroxyl groups (—OH), and the O—C=O groups corresponded to the carboxyl groups (—COOH) [17], which is pertinent to the surface functional groups. Among all the samples, F-MAC showed the largest intensity area of oxygen-related functional groups due to the large specific surface area. In addition, the C-F groups of F-PC and F-MAC were detected at ~ 291.2 eV because of fluorine impregnation [18]. In the enlarged XPS data shown in **Fig. 2b**, it can be seen that the C-F groups of F-MAC were increased due to the synergistic effect of fluorine impregnation and KOH activation compared with that of F-PC. In the F 1 s XPS core-level spectra (**Fig. 2c**), F-C groups were detected at ~ 689 eV, thus exhibiting the same tendency as that of the C 1 s core-level spectra [19]. As shown in the summarized binding ratio for the C 1 s core-level spectra (**Fig. 2d**), F-MAC had the lowest ratio of C—C groups (51.3%) and the highest ratio of oxygen-related functional groups (including C—O, C=O, and O—C=O groups) (44.4%) and F-C groups

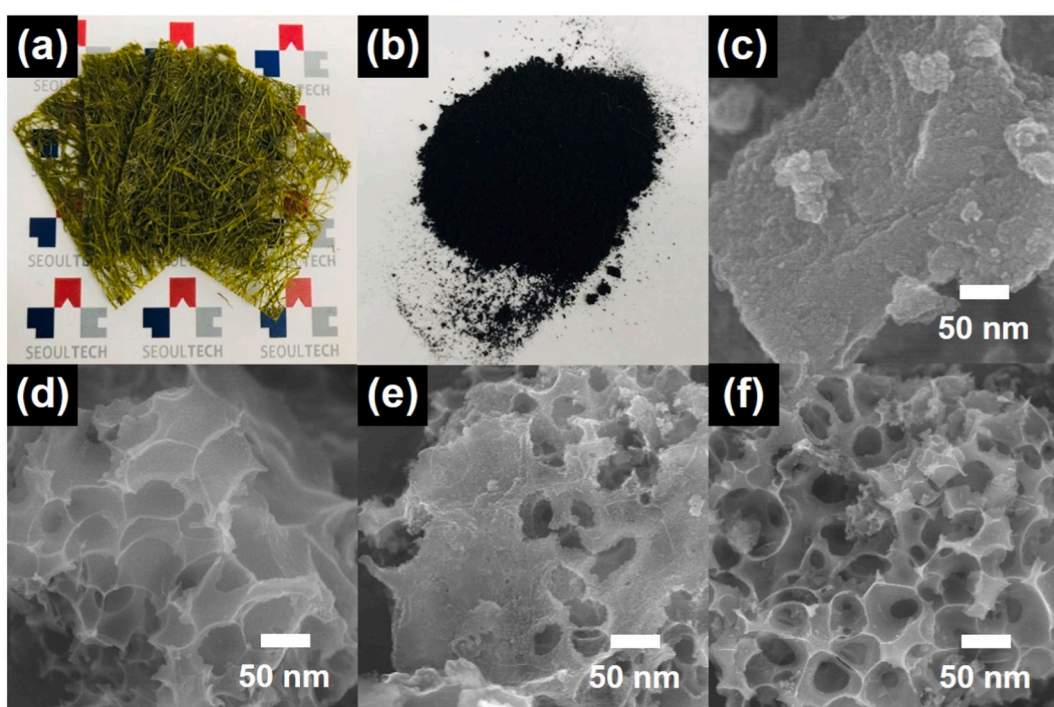


Fig. 1. Images of (a) dried EC, (b) carbonized F-MAC and FESEM images of (c) PC, (d) AC, (e) F-PC, and (f) F-MAC samples.

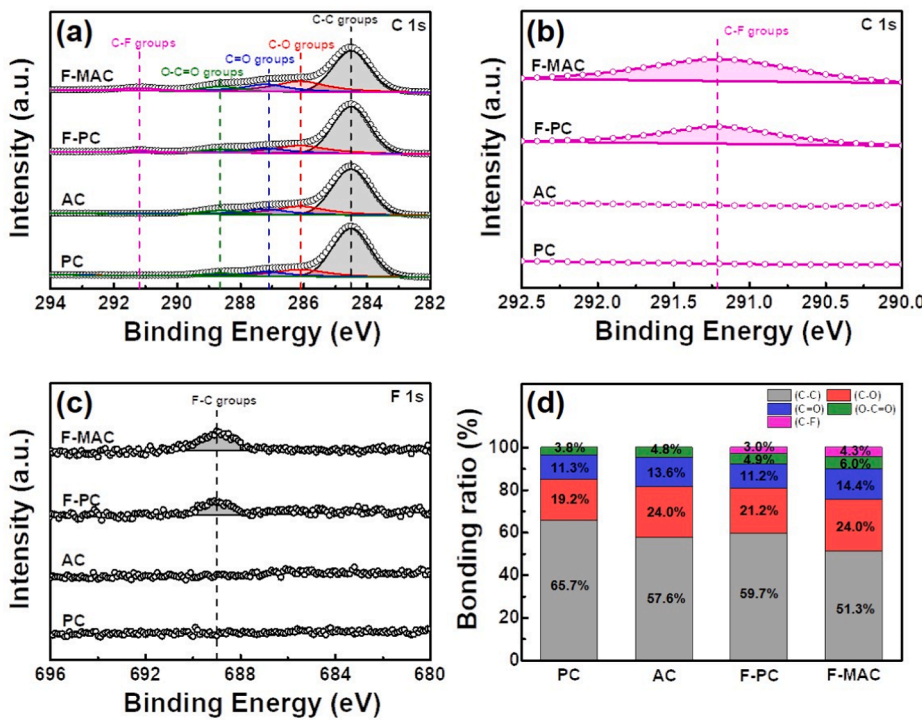


Fig. 2. XPS core-level spectra of (a) C 1s, (b) enlarged C 1s, and (c) F 1s and (d) chemical bonding ratio obtained from PC, AC, F-PC, and F-MAC.

(4.3%). This result indicates that the concurrent application of fluorine impregnation and KOH activation can effectively break the C-C bonding, develop a mesoporous structure with a large number of oxygen functional groups, and facilitate the fluorine doping process. This unique strategy improved the mesopore structure by providing a large number of surface oxygen functional groups, and the fluorine doping contributed to the improved energy storage performance by providing enhanced electrolyte wettability and electrical conductivity [20,21].

Fig. 3 shows the BET and BJH data obtained using N₂ adsorption/desorption isotherms to characterize the pore structures of all samples. Generally, pores can be categorized into three types according to the pore size: micropores (<2 nm), mesopores (2–50 nm), and macropores (>50 nm) [22,23]. In Fig. 3a, the PC curve indicates typical bulk behavior without pores and small specific surface area of 563 m²/g. The AC curve indicates type I behavior, corresponding to the presence of micropores, and a large surface area of 2287 m²/g. However, the curves of F-PC and F-MAC show type IV behavior (at P/P₀ > 0.4), corresponding to the mesoporous structure. In particular, F-MAC exhibited the optimized specific surface area of 2,710 m²/g due to the largest micropore volume of 1.387 cm³/g compared with the other samples (1.159 cm³/g for AC and 1.018 cm³/g for F-PC), which leads to the enhanced specific capacitance with enlarged active area [24]. In

addition, F-MAC exhibited a high mesopore volume fraction of 39% (see Fig. 3b) compared to AC and F-PC; this enhanced the high-rate performance by shortening the ionic diffusion pathway [25].

To investigate the electrochemical features, cyclic voltammetry (CV) measurements were carried out at a scan rate of 10 mV/s (Fig. 4a). All the samples showed a rectangular CV curve, signifying the existence of a typical electrical double-layer area. F-MAC had the largest CV curve due to the increased specific capacitance, which implies an improvement in the electrochemical active area. Fig. 4b shows the summarized specific capacitance values of all samples, illustrating the energy storage performance at a current density of 0.2–20 A/g. PC, AC, F-PC, and F-MAC exhibited specific capacitances of 61, 163, 95, and 184 F/g, respectively, at a low current density of 0.2 A/g and 29, 122, 66, and 155 F/g, respectively, at a high current density of 20 A/g. This excellent capacitance value of F-MAC is due to the increased specific surface area and high oxygen functional group concentration. Furthermore, F-MAC showed excellent capacitance retention (85.1%) due to the increased mesopore volume fraction and enhanced electrical conductivity resulting from F-doping [26,27]. Fig. 4c shows the energy density and power density of the PC, AC, F-PC, and F-MAC with a Ragone plot calculated using specific capacitance values. The PC, AC, and F-PC showed the energy density of 7.6–4.4 W h/kg, 20.5–16.8 W h/kg, and 11.9–8.7 W h/

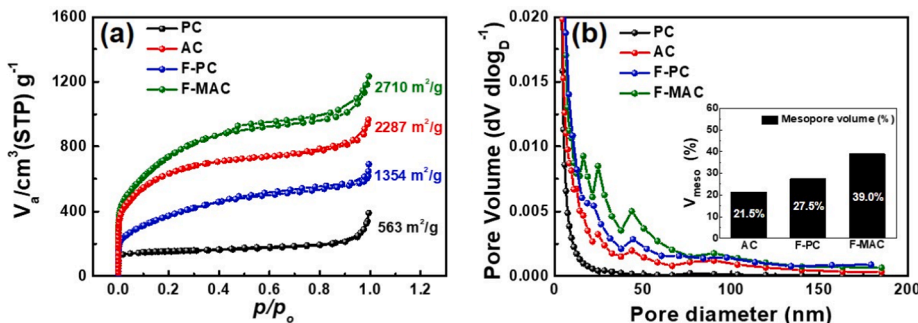


Fig. 3. (a) BET N₂ adsorption and desorption isotherms and (b) BJH pore size distribution of PC, AC, F-PC, and F-MAC.

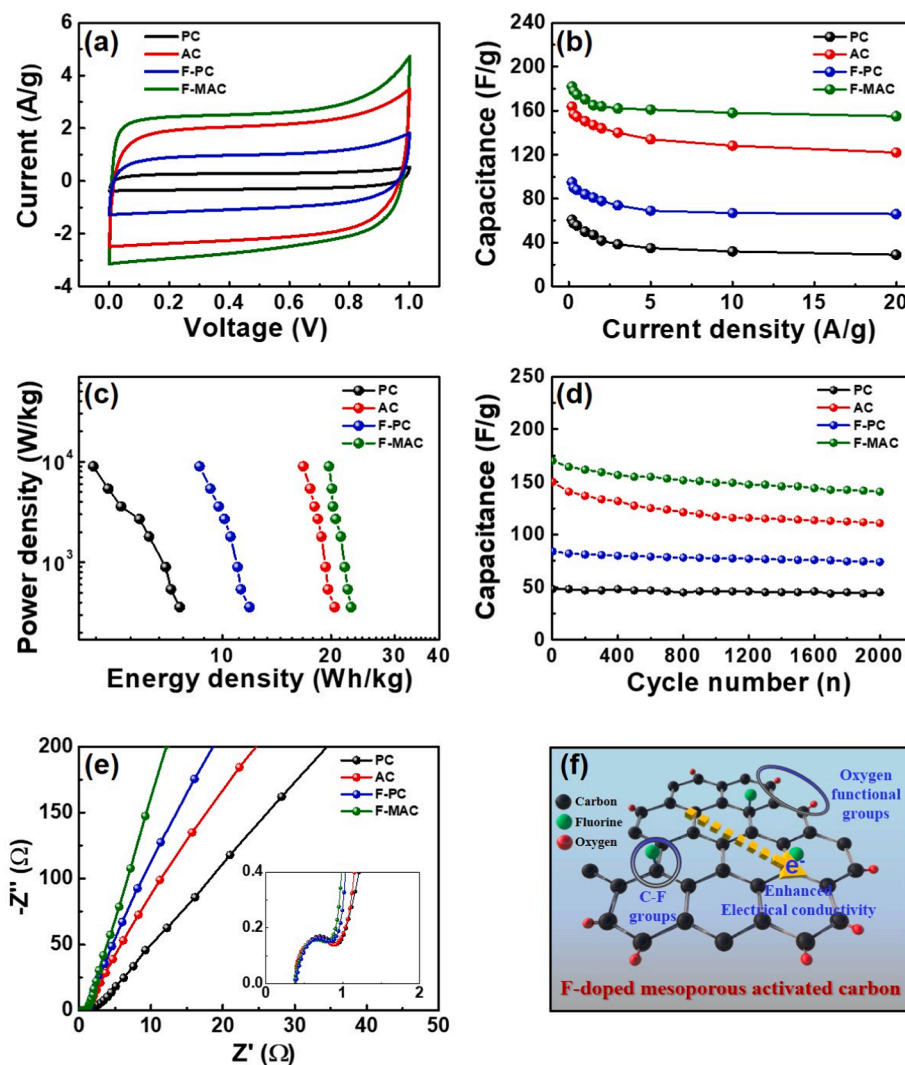


Fig. 4. (a) CV curves examined from 0 V to 1 V at the scan rate of 10 mV/s, (b) specific capacitance values at a current density of 0.2–20 A/g, (c) Ragone plots related to energy and power densities, (d) cycle stability up to 2000 cycles at a current density of 1 A/g, (e) Nyquist plots at the open circuit potential obtained from PC, AC, F-PC, and F-MAC, and (f) schematic illustration of the lattice structure of F-MAC.

kg at a power density range of 360–9000 W/kg, respectively. And as expected, F-MAC showed the highest energy density of 22.8–19.8 Wh/kg at the same power density of 360–9000 W/kg. To evaluate the cycle stability, consecutive charging/discharging tests were conducted for up to 2000 cycles at a current density of 1 A/g (Fig. 4d). F-MAC exhibited superior cycle stability with a capacitance retention of 82.8% after 2000 cycles. This result is attributed to the optimized mesoporous structure and increased oxygen functional groups. First, the optimized mesoporous structure can improve the cycling stability with short ion diffusion distance. This decreased ion diffusion distance effectively enhances the ion transfer efficiency during charge/discharge cycles, which enables stable long-term stability [28]. Second, the increased oxygen-functional groups of carbon surface provide the enhanced inner wettability and electronegativity of active material, which can make ion easier to enter into the deeper pores of active material, leading to an increased surface pore utilization rate [29]. The enhanced pore utilization rate can facilitate the effect of mesopore regarding the cycle stability. Further, in the Nyquist plots shown in Fig. 4e, F-MAC has the largest inclined line slope (at a low-frequency area) and the smallest semicircle (at a high-frequency area), which implies a superior ionic diffusion rate and high electrical conductivity, respectively [30]. Fig. 4f shows the schematic illustration of lattice structure of F-MAC, possessing the oxygen functional groups and C-F groups.

Thus, the superior electrochemical performance of F-MAC can be attributed to the following factors: First, the increased specific surface area resulted in a high specific capacitance at a low current density. Second, the optimized mesoporous structure and F-doping into carbon provided favorable ionic transfer pathways and enhanced the electrical conductivity, resulting in an increased high-rate performance. Third, a high concentration of oxygen functional groups contributed to improved cycle stability due to the increased electrolyte wettability.

4. Conclusion

In this study, F-MAC was synthesized via the synergistic effect of fluorine impregnation and KOH activation process. F-MAC reported the high specific surface area of $2710\text{ m}^2/\text{g}$ and increased mesopore volume fraction of 39% via a carbon fluoride generation/decomposition process during carbonization. F-MAC exhibited excellent electrochemical performance with a high specific capacitance of 184 F/g, high-rate performance of 155 F/g at a current density of 20 A/g, and capacitance retention of 82.8% after 2000 cycles. This can be attributed to the following factors: (1) the high specific surface area resulting from the fluorine impregnation and KOH activation provided high specific capacitance at a low current density; (2) the enhanced mesoporous structure and F-doping into the carbon led to superior high-rate

performance with high cycling stability; and (3) the high concentration of oxygen functional groups provided improved cycle stability. Therefore, F-MAC can be considered as a good candidate for high-performance EDLCs.

CRediT authorship contribution statement

Kue-Ho Kim: Conceptualization, Methodology, Investigation, Writing - original draft. **Jung-Soo Lee:** Methodology. **Hyo-Jin Ahn:** Conceptualization, Supervision, Writing - review & editing.

Declaration of Competing Interest

The authors declare that they have no known competing financial interests or personal relationships that could have appeared to influence the work reported in this paper.

Acknowledgements

This work was supported by the National Research Foundation of Korea (NRF) grant funded by the Korea government (MSIT) (No. 2019R1A2 C1005836).

References

- [1] W. Raza, F. Ali, N. Raza, Y. Luo, K.-H. Kim, J. Yang, S. Kumar, A. Mehmood, E. Kwon, Recent advancements in supercapacitor technology, *Nano Energy* 52 (2018) 441–473.
- [2] S. Faraji, F.N. Ani, The development supercapacitor from activated carbon by electroless plating—A review, *Renew. Sust. Energ. Rev.* 42 (2015) 823–834.
- [3] B. Liu, R. Shi, R. Chen, C. Wang, K. Zhou, Y. Ren, Z. Zeng, Y. Liu, L. Li, Optimized synthesis of nitrogen-doped carbon with extremely high surface area for adsorption and supercapacitor, *Appl. Surf. Sci.* 538 (2021) 147961.
- [4] J.R. Miller, Perspective on electrochemical capacitor energy storage, *Appl. Surf. Sci.* 460 (2018) 3–7.
- [5] P. Simon, Y. Gogotsi, Materials for electrochemical capacitors, *Nat. Mater.* 7 (2008) 845–854.
- [6] R.-J. Mo, Y. Zhao, M. Wu, H.-M. Xiao, S. Kuga, Y. Huang, J.-P. Li, S.-Y. Fu, Activated carbon from nitrogen rich watermelon rind for high-performance supercapacitors, *RSC Adv.* 6 (2016) 59333–59342.
- [7] I.I.G. Inal, S.M. Holmes, A. Banford, Z. Aktas, The performance of supercapacitor electrodes developed from chemically activated carbon produced from waste tea, *Appl. Surf. Sci.* 357 (2015) 696–703.
- [8] M.S. Balathangaimani, W.-G. Shim, M.-J. Lee, C. Kim, J.-W. Lee, H. Moon, Highly porous electrodes from novel corn grains-based activated carbons for electrical double layer capacitors, *Electrochim. Commun.* 10 (2008) 868–871.
- [9] J. Mi, X.-R. Wang, R.-J. Fan, W.-H. Q, W.-C. Li, Coconut-shell-based porous carbons with a tunable micro/mesopore ratio for high-performance supercapacitors, *Energy Fuels* 26 (2012) 5321–5329.
- [10] K. Sun, S. Yu, Z. Hu, Z. Li, G. Lei, Q. Xiao, Y. Ding, Oxygen-containing hierarchically porous carbon materials derived from wild jujube pit for high-performance supercapacitor, *Electrochim. Acta* 231 (2017) 417–428.
- [11] Z. Teng, K. Han, J. Li, Y. Gao, M. Li, T. Ji, Ultrasonic-assisted preparation and characterization of hierarchical porous carbon derived from garlic peel for high-performance supercapacitors, *Ultrason. Sonochem.* 60 (2020) 104756.
- [12] W. Yu, H. Wang, S. Liu, N. Mao, X. Liu, J. Shi, W. Liu, S. Chen, X. Wang, N. O-codoped hierarchical porous carbons derived from algae for high-capacity supercapacitors and battery anodes, *J. Mater. Chem. A* 4 (2016) 5973–5983.
- [13] H. Zhang, Z. Mo, R. Guo, N. Liu, M. Yan, R. Wang, H. Feng, X. Wei, Facile preparation of three-dimensional honeycomb nitrogen-doped carbon materials for supercapacitor applications, *J. Mater. Res. Symp.* 34 (2019) 1200–1209.
- [14] K.-H. Kim, D.-Y. Shin, H.-J. Ahn, Ecklonia cava based mesoporous activated carbon for high-rate energy storage devices, *J. Ind. Eng. Chem.* 84 (2020) 393–399.
- [15] G. Chen, Z. Shi, J. Yu, Z. Wang, J. Xu, B. Gao, X. Hu, Kinetic analysis of the non-isothermal decomposition of carbon monofluoride, *Thermochim. Acta* 589 (2014) 63–69.
- [16] Y. Sato, K. Itoh, R. Hagiwara, T. Fukunaga, Y. Ito, Short-range structures of poly (dicarbon monofluoride) (C_2F_n) and poly(carbon monofluoride) (CF)_n, *Carbon* 42 (2004) 2897–2903.
- [17] G.-H. An, H.-J. Ahn, Surface modification of RuO₂ nanoparticles–carbon nanofiber composites for electrochemical capacitors, *J. Electroanal. Chem.* 744 (2015) 32–36.
- [18] J. Guo, J. Zhang, H. Zhao, Y. Fang, K. Ming, H. Huang, J. Chen, X. Wang, Fluorine-doped graphene with an outstanding electrocatalytic performance for efficient oxygen reduction reaction in alkaline solution, *R. Soc. Open Sci.* 5 (2018) 180925.
- [19] H. Wang, A. Kong, Mesoporous fluorine-doped carbon as efficient cathode material for oxygen reduction reaction, *Mater. Lett.* 136 (2014) 384–387.
- [20] H. Geng, H. Ming, D. Ge, J. Zheng, H. Gu, Designed fabrication of fluorine-doped carbon coated mesoporous TiO₂ hollow spheres for improved lithium storage, *Electrochim. Acta* 157 (2015) 1–7.
- [21] G.-H. An, D.-Y. Lee, H.-J. Ahn, Hierarchically mesoporous activated carbon prepared from the dissolution of zinc oxide for high-rate electrical double layer capacitors, *J. Ind. Eng. Chem.* 65 (2018) 423–428.
- [22] E. Raymundo-Pinero, F. Leroux, F. Béguin, A high-performance carbon for supercapacitors obtained by carbonization of a seaweed biopolymer, *Adv. Mater.* 18 (2006) 1877–1882.
- [23] C. Largeot, C. Portet, J. Chmiola, P.-L. Taberna, Y. Gogotsi, P. Simon, Relation between the ion size and pore size for an electric double-layer capacitor, *J. Am. Chem. Soc.* 130 (2008) 2730–2731.
- [24] C. Yang, Q. Pan, Q. Jia, Y. Xin, W. Qi, H. Wei, S. Yang, B. Cao, Multifunctional microporous activated carbon nanotubes anchored on graphite fibers for high-strength and high-rate flexible all-solid-state supercapacitors, *Appl. Surf. Sci.* 502 (2020) 144423.
- [25] G.-H. An, Ultrafast long-life zinc-ion hybrid supercapacitors constructed from mesoporous structured activated carbon, *Appl. Surf. Sci.* 530 (2020) 147220.
- [26] G.-H. An, B.-R. Koo, H.-J. Ahn, Activated mesoporous carbon nanofibers fabricated using water etching-assisted templating for high-performance electrochemical capacitors, *Phys. Chem. Chem. Phys.* 18 (2016) 6587–6594.
- [27] C. Wang, J. Wang, W. Wu, J. Qian, S. Song, Z. Yue, Feasibility of activated carbon derived from anaerobic digester residues for supercapacitors, *J. Power Sources* 412 (2019) 683–688.
- [28] Q. Wang, J. Yan, T. Wei, J. Feng, Y. Ren, Z. Fan, M. Zhang, X. Jing, Two-dimensional mesoporous carbon sheet-like framework material for high-rate supercapacitors, *Carbon* 60 (2013) 481–487.
- [29] X.-R. Li, Y.-H. Jiang, P.-Z. Wang, Y. Mo, W.-D. Lai, Z.-J. Li, R.-J. Yu, Y.-T. Du, X.-R. Zhang, Y. Chen, Effect of the oxygen functional groups of activated carbon on its electrochemical performance for supercapacitors, *New Carbon Mater.* 35 (2020) 232–243.
- [30] K.-H. Kim, S.-J. Jung, B.-R. Koo, H.-J. Ahn, Surface amending effect of N-doped carbon-embedded NiO films for multilayer electrochromic energy-storage devices, *Appl. Surf. Sci.* 537 (2021) 147902.